GEOLOGY | THE GEOLOGICAL SOCIETY OF AMERICA®

https://doi.org/10.1130/G50556.1

Manuscript received 5 July 2022
Revised manuscript received 16 September 2022
Manuscript accepted 29 September 2022

Published online 20 December 2022

Late Miocene to recent tectonic evolution of the Macquarie Triple Junction

Luca Gasperini[1]*, Marco Ligi[1], Daniela Accettella[2], Alessandro Bosman[3], Marco Cuffaro[3], Emanuele Lodolo[2], Eleonora Martorelli[3], Filippo Muccini[3,4], Camilla Palmiotto[1] and Alina Polonia[1]

[1]Istituto di Scienze Marine, CNR, 40129 Bologna, Italy
[2]Istituto Nazionale di Oceanografia e di Geofisica Sperimentale, 34010 Trieste, Italy
[3]Istituto di Geologia Ambientale e Geoingegneria, CNR, 00185 Rome, Italy
[4]Istituto Nazionale di Geofisica e Vulcanologia, 00143 Rome, Italy

ABSTRACT

The Pacific, Antarctic, and Macquarie lithospheric plates diverge from the Macquarie Triple Junction (MTJ) in the southwestern Pacific Ocean, south of Macquarie Island. Morphobathymetric, magnetic, and gravity data have been used to understand the evolution of the three accretionary/transform boundaries that meet at the MTJ. Plate velocities, estimated near the MTJ and averaged over the past 3 m.y., indicate an unstable ridge–fault–fault triple junction. The long life (>6 m.y.) of this configuration can be attributed to a rapid increase in spreading asymmetry along the Southeast Indian Ridge segment as it approaches the MTJ, and to transtension along the southernmost strand of the Macquarie–Pacific transform boundary. A major change in plate motion triggered the development of the Macquarie plate at ca. 6 Ma and makes clear the recent evolution of the MTJ, including (1) shortening of the Southeast Indian Ridge segment; (2) formation of the westernmost Pacific-Antarctic Ridge, which increased its length over time; and (3) lengthening of the two transform boundaries converging in the MTJ. The clockwise change of the Pacific-Antarctic motion (ca. 12–10 Ma) led to complex geodynamic evolution of the plate boundary to the east of the triple junction, with fragmentation of the long-offset Emerald transform fault and its replacement over a short time interval (1–2 m.y.) with closely spaced, highly variable transform offsets that were joined by short ridge segments with time-varying asymmetries in the spreading rates.

INTRODUCTION

In the theory of plate tectonics, which approximates each plate as a rigid spherical shell, each plate boundary must be a continuous curve, and any branch in this curve is called a triple junction, which implies the presence of a third plate. Plate boundary geometries and relative plate velocities control the kinematic stability of a triple junction, defined by its ability to retain its geometry over time (McKenzie and Morgan, 1969; Patriat and Courtillot, 1984; Searle and Francheteau, 1986). The very few triple junctions on Earth involving only accretionary and conservative margins, such as the Galapagos (eastern Pacific Ocean), Bouvet (South Atlantic Ocean), Rodriguez (Indian Ocean), and Macquarie (southern Pacific Ocean) triple junctions, are marked by complex, poorly understood interactions of the plate boundaries and display a more complex geologic history than their long-term kinematic stability may suggest (Mitchell, 1991; Ligi et al., 1997, 1999; Mitchell and Livermore, 1998; Bird et al., 1999; Viso et al., 2005; Schouten et al., 2008; Choi et al., 2017).

In the western Pacific, at ca. 48 Ma, a major plate reorganization formed a triple junction between the Australian, Pacific, and Antarctic plates; then Australia split into Australia and Macquarie at ca. 6 Ma, and today the Macquarie, Pacific, and Antarctic plates meet at the Macquarie Triple Junction (MTJ), south of Macquarie Island (Fig. 1; Massell et al., 2000; Meckel et al., 2003; Cande and Stock, 2004, Lodolo et al., 2013).

Our understanding of the plate kinematics in this region is mostly based on magnetic anomalies and plate boundary reconstructions (Falconer, 1972; Cande et al., 1995; Sutherland, 1995; Lamarche et al., 1997; Cande and Stock, 2004; Croon et al., 2008).

Based on a compilation of high-resolution morphobathymetric, magnetic, and gravity data, we reconstructed the kinematics and neotectonics of the MTJ region, including the triple junction configuration and its long-term stability.

TECTONIC FRAMEWORK

Initially, the Australia–Pacific–Antarctic triple junction was located at the end of the easternmost Southeast Indian Ridge spreading segment, and was connected eastward to the spreading segment of the Pacific-Antarctic Ridge by the 450-km-long offset Emerald transform fault (Marks and Stock, 1997). Plate reconstructions show that since 33 Ma, the triple junction has migrated southward with respect to the Australian plate, resulting in the present-day curved plate boundary (Cande and Stock, 2004). The triple junction migration led to shortening of the easternmost Southeast Indian Ridge segment, lengthening of the left-lateral Emerald transform fault (Croon et al., 2008) to ~1200 km between magnetic chrons 6C and 5o (24.1–10.95 Ma), and lengthening of the dextral transform fault that represents the southern end of the Australian–Pacific plate boundary. Before chron 5o, the latter changed from a dextral transform fault into an obliquely convergent zone of incipient subduction in the Hjort region (Meckel et al., 2003). At ca. 6 Ma, another change in the motion of the Australia and Pacific plates relative to Antarctica triggered the development of the Macquarie plate, and the recent ridge–fault–fault (RFF) evolution of the MTJ (Cande and Stock, 2004; Choi et al., 2017). Thus, the evolution of the triple junction since the Oligocene has involved stages of RFF, ridge–trench–fault, and then a return to RFF configurations, with highly variable geometry of the accretionary/transform boundaries (Croon et al., 2008).

*E-mail: luca.gasperini@bo.ismar.cnr.it

CITATION: Gasperini, L., et al., 2023, Late Miocene to recent tectonic evolution of the Macquarie Triple Junction: Geology, v. XX, p. , https://doi.org/10.1130/G50556.1

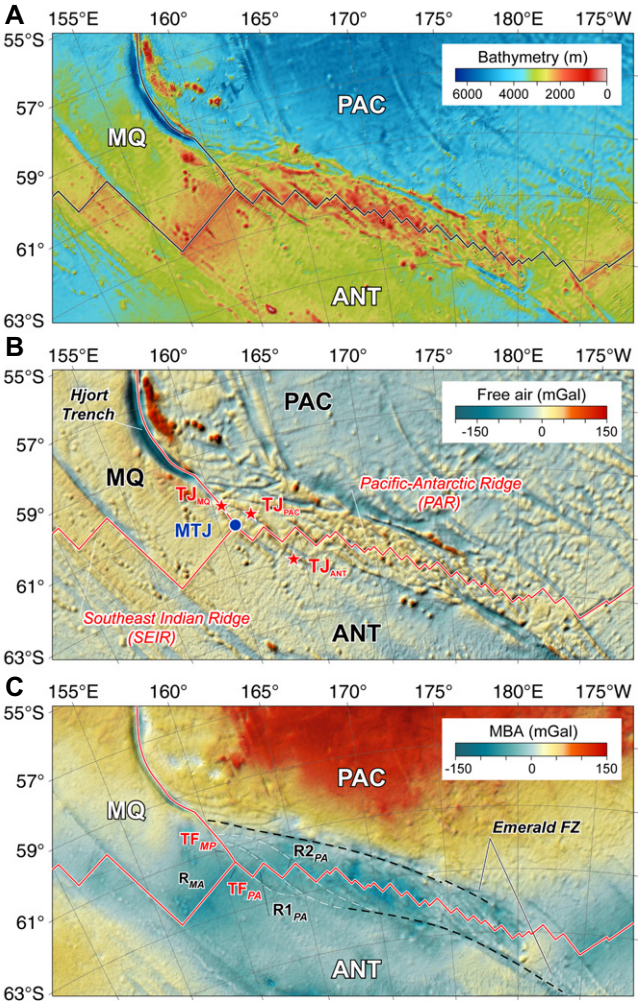

Figure 1. (A) A synthesis of multibeam bathymetric data from the southwestern Pacific, including our own, those of Crowley et al. (2015), and of the U.S. National Oceanic and Atmospheric Administration's National Geophysical Data Center (NGDC) database (https://www.ncei.noaa.gov/-maps/bathymetry/) merged with the General Bathymetric Chart of the Oceans (GEBCO) 2021 grid (https://doi.org/10.5285/c6612cbe-50b3-0cff-e053-6c86abc09f8f). Black solid lines indicate plate boundaries between the Australian (MQ), Pacific (PAC), and Antarctic (ANT) plates. (B) Satellite-derived, free-air anomalies from the 1-arc-min global grid (v. 31; https://topex.ucsd.edu/pub/-global_grav_1 min) of Sandwell et al. (2014). Red asterisks mark the former position of the Macquarie Triple Junction (MTJ) at the time when the Macquarie plate formed (ca. 6 Ma). Blue circle indicates the present-day MTJ location. (C) Mantle Bouguer anomaly (MBA). The grid was generated by subtracting the attraction of seafloor topography and the crust-mantle interface from free-air anomalies, assuming a 6-km-thick crust and densities of 1040, 2670, and 3330 kg m^{-3} for seawater, crust, and mantle, respectively. Red lines mark plate boundaries; black dashed lines indicate traces of the Emerald fracture zone (FZ); and white dashed line indicates the Pacific-Antarctic Ridge fracture zones next to the MTJ. R_{MA}—Macquarie–Antarctic ridge segment; TF_{MP}—Macquarie–Pacific transform boundary; TF_{PA}—Pacific–Antarctic transform boundary; $R1_{PA}$ and $R2_{PA}$—westernmost Pacific-Antarctic Ridge segments.

FIELD WORK

A problem with detailed kinematic reconstructions of the MTJ is that the region has remained under-investigated due to its remoteness. Only sparse surveys have been carried out since the early 1970s. In the 1990s, two expeditions with R/V *OGS Explora* within the Italian "Progetto Nazionale di Ricerche in Antartide" collected gravity, magnetic, and multichannel seismic data along sparse profiles across the Macquarie–Pacific–Antarctic plate boundaries next to the MTJ (Lodolo and Coren, 1997; Lodolo et al., 2013). More recently, high-resolution bathymetric and magnetic data were acquired by R/V *Araon* and M/V *L'Astrolabe* cruises along the axis of the two easternmost Southeast Indian Ridge segments (Crowley et al., 2015; Hahm et al., 2015; Choi et al., 2017).

In 2017 and 2019, onboard R/V *Explora* and R/V *Laura Bassi*, we carried out a series of multibeam and magnetic surveys focused on the three plate boundaries meeting at the MTJ: the Macquarie–Antarctic ridge segment (R_{MA}), the Pacific–Antarctic (TF_{PA}) transform boundary, and the Macquarie–Pacific (TF_{MP}) transform boundary. Multibeam bathymetric data were merged with those of Crowley et al. (2015) and the U.S. National Oceanographic and Atmospheric Administration's National Geophysical Data Center (NGDC) database (https://www.ncei.noaa.gov/-maps/bathymetry/). Seafloor digital elevation models and backscatter images were produced down to a horizontal resolution of 25 m (Fig. 2; Fig. S1 in the Supplemental Material[1]). Satellite-derived free-air gravity (Fig. 1B) and bathymetric data were used to calculate the mantle Bouguer anomaly (Fig. 1C).

[1]Supplemental Material. Tectonic setting of the southwestern Pacific Ocean including kinematics data. Please visit https://doi.org/10.1130/GEOL.S.21520953 to access the supplemental material, and contact editing@geosociety.org with any questions.

The Macquarie–Antarctic Ridge Segment

The ~300-km-long easternmost Southeast Indian Ridge segment (Fig. 1) constitutes the accretionary boundary between the Macquarie and Antarctic plates. Its axial morphology varies along strike: axial highs with local small axial valleys at an average depth of ~2000 m give way to a pronounced axial valley as the spreading ridge (R_{MA}) approaches the triple junction. The ridge axis strikes N59°E, and its eastern end deepens sharply to 2900 m in a 30-km-long, ~12–17-km-wide axial valley (Fig. 2A). Crustal fabric, with well-developed crests and valleys, shapes large parts of the seafloor adjacent to the ridge axis and determines the isochron trend (Fig. 2). On the southern side of R_{MA} (Antarctic plate), fabric lineaments run subparallel to the ridge up to 180 km from the axis (Fig. 2A). Conversely, on the Macquarie plate along the northern side of the R_{MA}, the oceanic fabric progressively rotates clockwise, from southwest-northeast to west-east, as it approaches the Macquarie–Pacific plate boundary, with increasing rotation moving away from the ridge axis. The magnetic Line B of Choi et al. (2017) intersects the central part of R_{MA} and provides full spreading rates of 64–66 mm/yr, which is relatively constant up to chron 3o (5.23 Ma) with symmetrical magnetic anomalies. Our magnetic Line 1 runs across the Macquarie–Antarctic boundary in the vicinity of the triple junction (Fig. 2A) and exhibits magnetic anomalies up to chron 3y (4.18 Ma) toward the north and to 2Ay (2.58 Ma) southward (Fig. 2B). Full spreading rates range from 57.5 mm/yr to 60 mm/yr, while the half spreading rates are strongly asymmetrical with faster accretion of the Antarctica plate. Estimated values averaged over the last 3.58 Ma (chron 2Ao) are 28.5 mm/yr and 31.4 mm/yr on the northern and southern side, respectively.

The Pacific–Antarctic Plate Boundary

The eastern end of the R_{MA} is linked southward through a small triangular nodal basin (3250 m deep) to the westernmost Pacific-Antarctic Ridge segment ($R1_{PA}$) by an 82 km-long, left-lateral transform fault (TF_{PA}). The transform valley is narrow at the ridge-transform intersections and widens (up to ~4 km) in its central part, with a maximum depth of 3937 m (Fig. 2C). The southern ridge-transform intersection is shallower, with depths of <~2000 m, and a nodal basin is missing. Well defined j-shaped features dominate both the inner and outer corners. The principal transform displacement zone appears narrow and focused on a single continuous fault, although a series of en-echelon strike-slip segments is observed in the center of the valley (Fig. 2B).

$R1_{PA}$ is the closest Pacific-Antarctic Ridge spreading segment to the MTJ and it is linked eastward to the next ridge segment ($R2_{PA}$) by

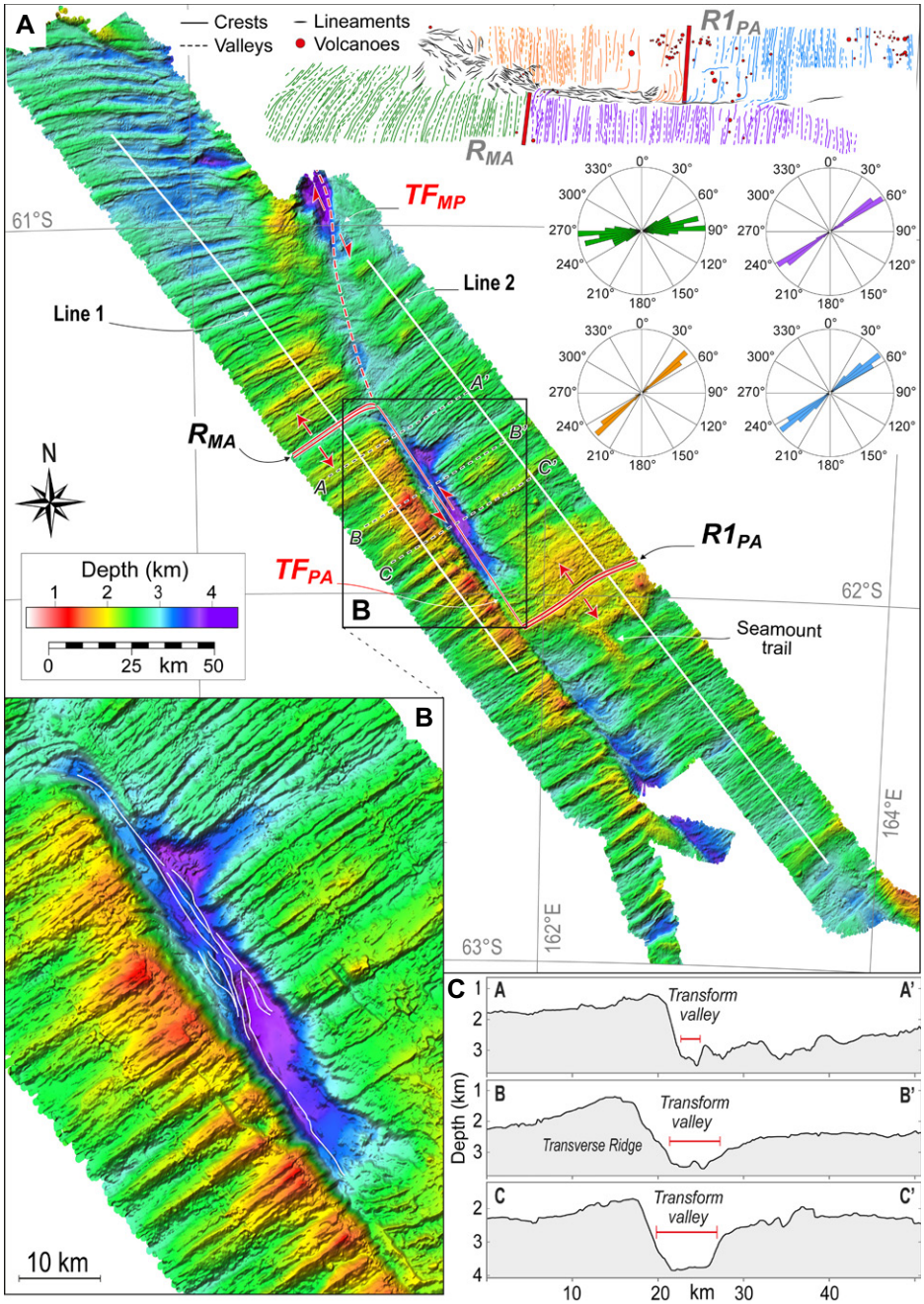

Figure 2. (A) Morphology of the Macquarie Triple Junction region from the new swath of bathymetric data. Red lines indicate plate boundaries. White lines indicate locations of the magnetic lines in Figure 3. Upper right panel shows results from crustal fabric analysis with lineament directions plotted in rose diagrams. Solid and dashed lines indicate crests and valleys; purple and blue colors indicate Antarctica plate lineaments; green indicates Macquarie; and orange indicates Pacific. R_{MA}—Macquarie–Antarctic ridge segment; TF_{MP}—Macquarie–Pacific transform boundary; TF_{PA}—Pacific–Antarctic transform boundary; $R1_{PA}$—westernmost Pacific-Antarctic Ridge segment. (B) Details of the Macquarie Triple Junction and the southern transform Antarctic–Pacific plate boundary (TF_{PA}). (C) Bathymetric profiles across TF_{PA}. Locations are indicated as dashed lines in panel A.

an ~85-km-long, left-lateral transform fault (Fig. 1; Fig. S1). $R1_{PA}$ is ~62 km long and oriented N56°E. It has a typical fast ridge morphology with a pronounced axial high that rises up to a depth of < 2000 m.

Regular oceanic fabric marked by a sequence of subparallel alternating crests and valleys flanks both sides of the ridge axis. Fabric orientations in the rose diagrams of Figure 2A show a good correlation on both plates, with average spreading directions of 329° N for the past 3.58 m.y. Magnetic Line 2, which orthogonally crosses the central sector of $R1_{PA}$ (Fig. 2A), provides full spreading rates that decrease from ~49 mm/yr to ~44 mm/yr up to chron 3y (4.18 Ma) and shows symmetrical anomalies (Fig. 3A). Morphological and free-air gravity maps (Fig. 1) allow us to limit the extent of the lithosphere accreted to the Pacific plate and generated at $R1_{PA}$ up to a distance of ~145 km from the axis. Seafloor generated at $R1_{PA}$ appears to be bounded by the trace of the triple junction to the southwest and by the trace of the transform fault linking $R1_{PA}$ to $R2_{PA}$ to the northeast (Figs. 1 and 4).

The Macquarie–Pacific Transform Boundary

A 240-km-long dextral transform system marks the eastern boundary of the Macquarie plate connecting the MTJ with the Hjort trench to the north. A deep (>4400 m) pull-apart basin divides the transform system into two strands (Figs. 1 and 4). The northern strike-slip segment is straight, with a narrow principal transform displacement zone; it extends southeastward (157° N) for 170 km from the Hjort trench up to the intersection with the trace of the $R1_{PA}$–$R2_{PA}$ transform fault (TJ_{MQ} in Figs. 1 and 4). The ~70-km-long southern strand displays a 10-km-wide complex shear zone. Its northern deep sector includes a 30-km-long transtensional fault that is oriented at 180°N, bounding the pull-apart basin to the east, while a shallower, diffuse shear zone (depth of 2800–3000 m) forms the southern part of the plate boundary that converges to the MTJ, which strikes 160°N through a small nodal basin ~3300 m deep.

DISCUSSION

The Triple Junction

High-resolution multibeam bathymetric and magnetic data from the MTJ region confirm that a present-day RFF configuration is compatible with the observed plate kinematics, as has been suggested by several authors (Falconer, 1972; Massell et al., 2000; Meckel et al., 2003; Cande and Stock, 2004; Croon et al., 2008; Lodolo et al., 2013; Choi et al., 2017). Estimated relative plate velocities, averaged over the past 3.58 m.y., are 59.9, 43.5, and 16.5 mm/yr, with azimuths of 329°N, 326°N, and 157°N, and describe the Macquarie and Pacific plate motion relative to a fixed Antarctica, and the Macquarie displacement with respect to a fixed Pacific, respectively (Fig. 4). These magnitudes and directions are similar to those predicted for the triple junction by the finite rotations of Cande and Stock (2004) and Choi et al. (2017). We reconstructed a stability diagram for the MTJ (Fig. 4B) following the methods proposed by McKenzie and Morgan (1969) and Patriat and Courtillot (1984). The MTJ is unstable (in the sense of McKenzie and Morgan [1969]) because it is not possible to determine a point in the velocity space corresponding to reference frames where the position of all three plate boundaries is fixed (Fig. 4B). However, the faster Antarctic plate accretion observed along the Southeast Indian Ridge segment, with a spreading asymmetry increasing rapidly toward the MTJ due to a clockwise rotation of the Macquarie plate relative to Australia (Choi et al., 2017), and transtension along the southernmost strand of the

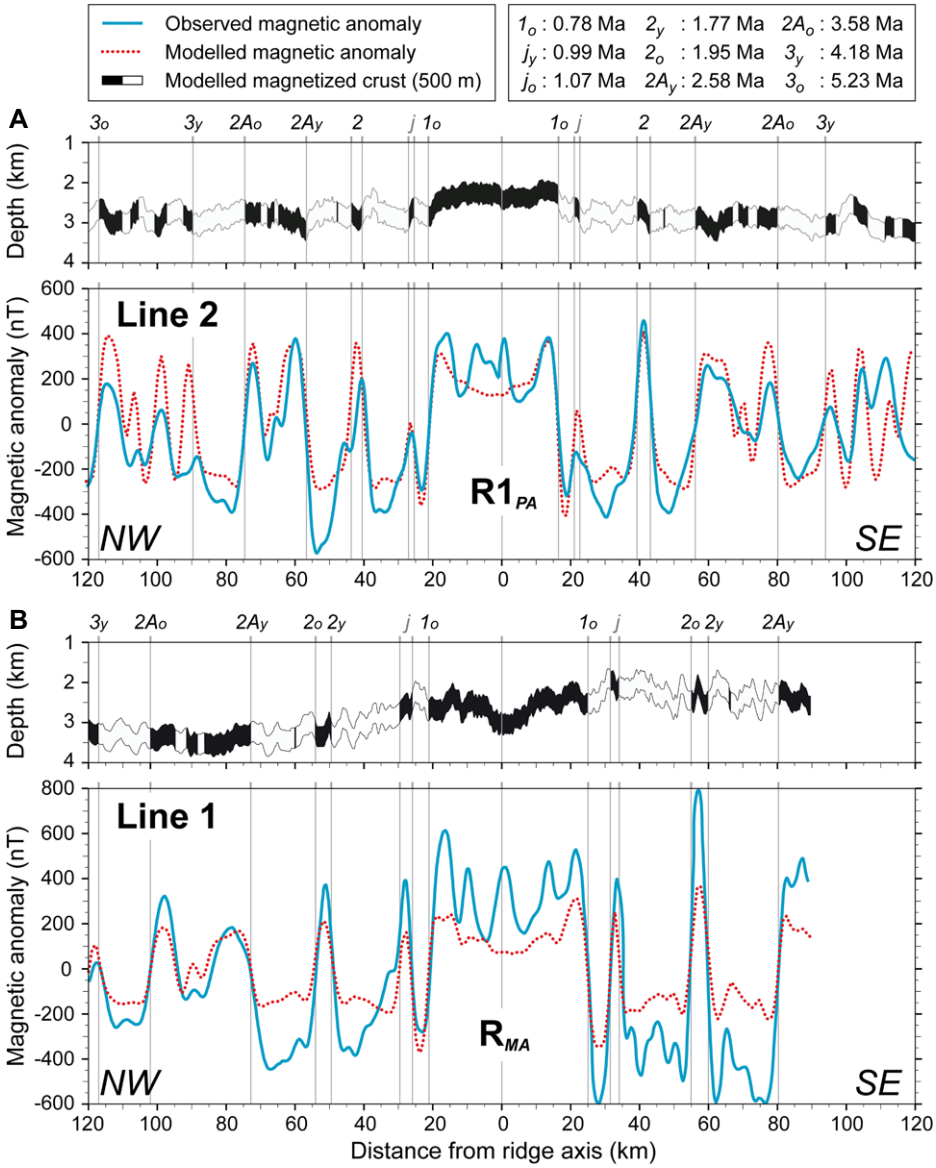

Figure 3. Geomagnetic reversal models of the magnetic lines of Figure 2. Top panels: geological model of magnetized crust assumed to be 0.5 km thick; Lower panels: observed magnetic anomalies (thick blue line) obtained by subtracting the International Geomagnetic Reference Field (IGRF)-13 from the raw data; dotted red line indicates modeled magnetic anomalies. Geomagnetic time scale is from Cande and Kent (1995). (A) Line 2 running across the central part of $R1_{PA}$ (the westernmost Pacific-Antarctic Ridge segment). (B) Line 1 intersecting the Macquarie–Antarctic ridge segment (R_{MA}) next to the triple junction.

Australian–Pacific boundary, allow the current MTJ configuration to persist.

Evolution of the Triple Junction

A sudden change in the Southeast Indian Ridge segment R_{MA} spreading direction between chrons 4A (8.86 Ma) and 3Ay (6.04 Ma) was observed by Choi et al. (2017) and interpreted as due to the formation of the Macquarie plate, as previously suggested by other authors (Cande and Stock, 2004; Austermann et al., 2011). We observed that the oldest terrains generated at the Pacific-Antarctic Ridge segment $R1_{PA}$ date back to 6.5 Ma (Fig. 4A). Therefore, a former RFF triple junction was located at the deep pull-apart basin (TJ_{MQ}, reference Macquarie plate; Figs. 1B and 4A), where the Southeast Indian Ridge segment R_{MA} was connected through a transform boundary to the Hjort trench in the north, and to the Pacific-Antarctic Ridge segment $R2_{PA}$ in the southeast. The major change in plate motion that triggered the development of the Macquarie plate also determined the recent evolution of the MTJ, which shifted to the present configuration due to the formation of a new Pacific-Antarctic Ridge segment ($R1_{PA}$) that increased its length over time at a rate of ~9.5 mm/yr. In the meantime, the Southeast Indian Ridge segment R_{MA} retreated at a rate of 4.5 mm/yr, and the northern (TF_{MP}) and southern (TF_{PA}) transform boundaries converging in the MTJ increased their lengths at a rate of ~10.8 mm/yr and ~12.3 mm/yr, respectively.

Numerical modeling predicts the development of wide, multi-fault transform boundaries in extra-long transform faults (Ligi et al., 2002) that may evolve toward intra-transform spreading centers, depending on the thermal state of the lithosphere (Maia et al., 2016). The clockwise change of the Pacific-Antarctic motion at ca. 12–10 Ma led to a complex geodynamic evolution of the plate boundary east of the MTJ (Cande et al., 1995; Wessel and Kroenke, 2008), with fragmentation of the long-offset Emerald transform fault (as shown by the mantle Bouguer anomaly; Fig. 1C). This transform was replaced in a relatively short time (1–2 m.y.; Fig. S2) by closely spaced, highly variable transform offsets joined by short ridge segments (Fig. 1) with time-varying asymmetries in spreading rates (Fig. S3).

Assuming that the plates were rigid, McKenzie and Morgan (1969; p. 126) suggested that "movement of stable junctions alone permits continuous plate evolution." However, by allowing for some local deformation at plate boundaries (i.e., local violation of the rigid plate assumption), even unstable triple junctions can constrain plate boundary evolution over the long-term.

ACKNOWLEDGMENTS

We thank Captain F. Sedmak and the officers and crew of R/V *OGS Explora* and R/V *Laura Bassi*; and E. Bonatti, P. Bird, and two anonymous reviewers for helpful and constructive comments. This work is dedicated to Marco and our amazing first trip to Antarctica.

REFERENCES CITED

Austermann, J., Ben-Avraham, Z., Bird, P., Heidbach, O., Schubert, G., and Stock, M.J., 2011, Quantifying the forces needed for the rapid change of Pacific plate motion at 6 Ma: Earth and Planetary Science Letters, v. 307, p. 289–297, https://doi.org/10.1016/j.epsl.2011.04.043.

Bird, R.T., Tebbens, S.F., Kleinrock, M.C., and Naar, D.F., 1999, Episodic triple-junction migration by rift propagation and microplates: Geology, v. 27, p. 911–914, https://doi.org/10.1130/0091-7613(1999)027<0911:Etriple junctionMBR>2.3.CO;2.

Cande, S.C., and Kent, D.V., 1995, Revised calibration of the geomagnetic polarity time scale for the Late Cretaceous and Cenozoic: Journal of Geophysical Research: Solid Earth, v. 100, p. 6093–6095, https://doi.org/10.1029/94JB03098.

Cande, S.C., and Stock, J.M., 2004, Pacific-Antarctic-Australia motion and the formation of the Macquarie Plate: Geophysical Journal International, v. 157, p. 399–414, https://doi.org/10.1111/j.1365-246X.2004.02224.x.

Cande, S.C., Raymond, C.A., Stock, J.M., and Haxby, W.F., 1995, Geophysics of the Pitman fracture zone and Pacific-Antarctic Plate motions during the Cenozoic: Science, v. 270, p. 947–953, https://doi.org/10.1126/science.270.5238.947.

Choi, H., Kim, S.-S., Dyment, J., Granot, R., Park, S.-H., and Hong, J.K., 2017, The kinematic evolution of the Macquarie Plate: A case study for the fragmentation of oceanic lithosphere: Earth and Planetary Science Letters, v. 478, p. 132–142, https://doi.org/10.1016/j.epsl.2017.08.035.

Croon, M.B., Cande, S.C., and Stock, J.M., 2008, Revised Pacific-Antarctic plate motions and geophysics of the Menard Fracture Zone:

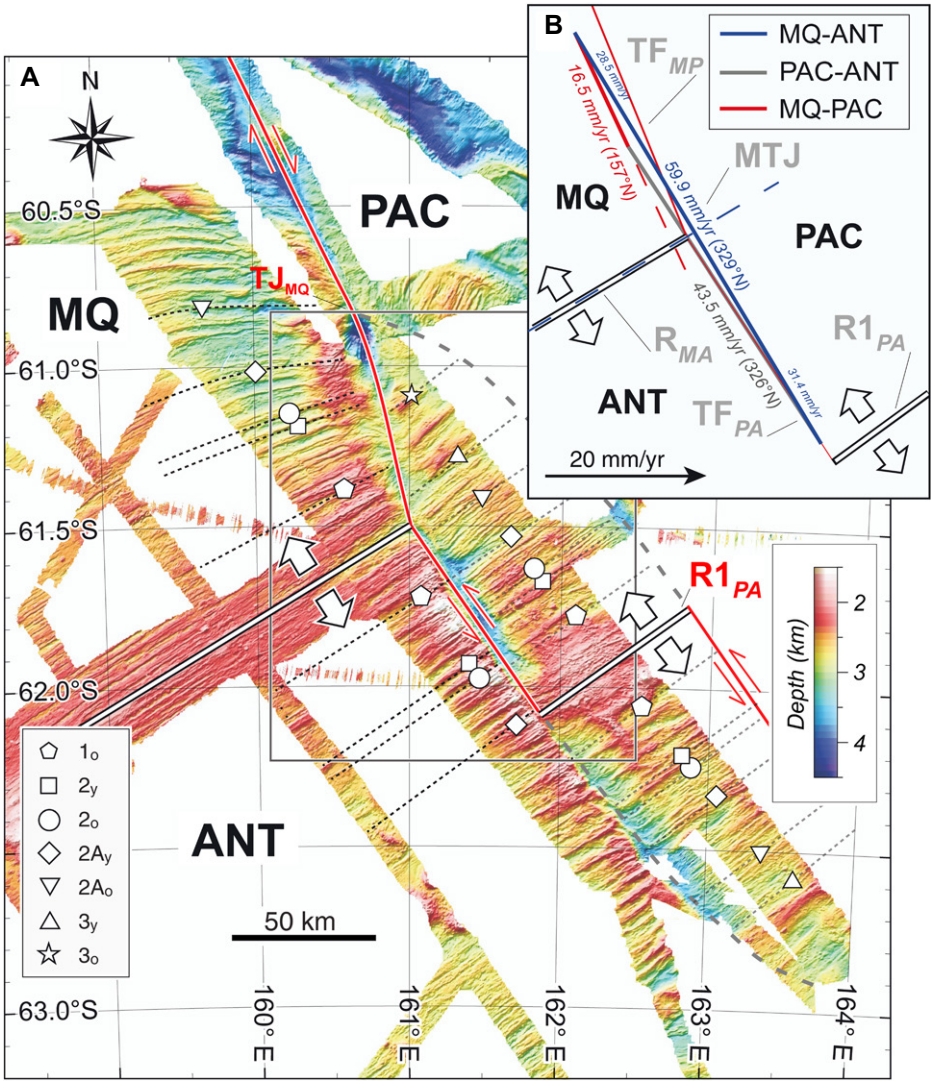

Figure 4. The Macquarie Triple Junction (MTJ). (A) Morphology, plate boundary geometry, and location of magnetic anomalies (empty symbols). Double black lines indicate mid-ocean ridges, and red lines indicate transform faults. Gray dashed lines follow the fracture zones and limit the lithosphere accreted at the westernmost Pacific-Antarctic Ridge segment ($R1_{PA}$). Plates: MQ—Australian; PAC—Pacific; ANT—Antarctica. (B) Present-day velocity triangle for the MTJ is compatible with an unstable ridge–fault–fault configuration. R_{MA}—Macquarie–Antarctic ridge segment; TF_{MP}—Macquarie–Pacific transform boundary; TF_{PA}—Pacific–Antarctic transform boundary; $R1_{PA}$—westernmost Pacific-Antarctic Ridge segment.

Geochemistry Geophysics Geosystems, v. 9, Q07001, https://doi.org/10.1029/2008GC002019.

Crowley, J.W., Katz, R.F., Huybers, P., Langmuir, C.H., and Park, S.-H., 2015, Glacial cycles drive variations in the production of oceanic crust: Science, v. 347, p. 1237–1240, https://doi.org/10.1126/science.1261508.

Falconer, R.K.H., 1972, The Indian–Antarctic–Pacific triple junction: Earth and Planetary Science Letters, v. 17, p. 151–158, https://doi.org/10.1016/0012-821X(72)90270-1.

Hahm, D., Baker, E.T., Rhee, T.S., Won, Y.-J., Resing, J.A., Lupton, J.E., Lee, W.-K., Kim, M., and Park, S.-H., 2015, First hydrothermal discoveries on the Australian–Antarctic Ridge: Discharge sites, plume chemistry, and vent organisms: Geochemistry Geophysics Geosystems, v. 16, p. 3061–3075, https://doi.org/10.1002/2015GC005926.

Lamarche, G., Collot, J.-Y., Wood, R.A., Sosson, M., Sutherland, R., and Delteil, J., 1997, The Oligocene–Miocene Pacific–Australia plate boundary, south of New-Zealand: Evolution from oceanic spreading to strike-slip faulting: Earth and Planetary Science Letters, v. 148, p. 129–139, https://doi.org/10.1016/S0012-821X(97)00026-5.

Ligi, M., Bonatti, E., Bortoluzzi, G., Carrara, G., Fabretti, P., Penitenti, D., Gilod, D., Peyve, A.A., Skolotnev, S., and Turko, N., 1997, Death and transfiguration of a triple junction in the South Atlantic: Science, v. 276, p. 243–245, https://doi.org/10.1126/science.276.5310.243.

Ligi, M., Bonatti, E., Bortoluzzi, G., Carrara, G., Fabretti, P., Gilod, D., Peyve, A.A., Skolotnev, S., and Turko, N., 1999, Bouvet Triple Junction in the South Atlantic: Geology and evolution: Journal of Geophysical Research: Solid Earth, v. 104, p. 29,365–29,385, https://doi.org/10.1029/1999JB900192.

Ligi, M., Bonatti, E., Gasperini, L., and Poliakov, A.N.B., 2002, Oceanic broad multifault transform plate boundaries: Geology, v. 30, p. 11–14, https://doi.org/10.1130/0091-7613(2002)030<0011:OBMTPB>2.0.CO;2.

Lodolo, E., and Coren, F., 1997, A Late Miocene plate boundary reorganization along the westernmost Pacific-Antarctic Ridge: Tectonophysics, v. 274, p. 295–305, https://doi.org/10.1016/S0040-1951(97)00005-X.

Lodolo, E., Coren, F., and Ben-Avraham, Z., 2013, How do long-offset oceanic transforms adapt to plate motion changes? The example of the Western Pacific–Antarctic plate boundary: Journal of Geophysical Research: Solid Earth, v. 118, p. 1195–1202, https://doi.org/10.1002/jgrb.50109.

Maia, M., et al., 2016, Extreme mantle uplift and exhumation along a transpressive transform fault: Nature Geoscience, v. 9, p. 619–623, https://doi.org/10.1038/ngeo2759.

Marks, K.M., and Stock, J.M., 1997, Early Tertiary gravity field reconstructions of the southwest Pacific: Earth and Planetary Science Letters, v. 152, p. 267–274, https://doi.org/10.1016/S0012-821X(97)00139-8.

Massell, C., Coffin, M.F., Mann, P., Mosher, S., Frohlich, C., Duncan, C.S., Karner, G., Ramsay, D., and Lebrun, J.-F., 2000, Neotectonics of the Macquarie Ridge Complex, Australia–Pacific plate boundary: Journal of Geophysical Research: Solid Earth, v. 105, p. 13,457–13,480, https://doi.org/10.1029/1999JB900408.

McKenzie, D., and Morgan, W.J., 1969, Evolution of triple junctions: Nature, v. 224, p. 125–133, https://doi.org/10.1038/224125a0.

Meckel, T.A., Coffin, M.F., Mosher, S., Symonds, P., Bernardel, G., and Mann, P., 2003, Underthrusting at the Hjort trench, Australian–Pacific plate boundary: Incipient subduction?: Geochemistry Geophysics Geosystems, v. 4, https://doi.org/10.1029/2002GC000498.

Mitchell, N.C., 1991, An evolving ridge system around the Indian Ocean triple junction: Marine Geophysical Researches, v. 13, p. 173–201, https://doi.org/10.1007/BF00369148.

Mitchell, N.C., and Livermore, R.A., 1998, The present configuration of the Bouvet Triple Junction: Geology, v. 26, p. 267–270, https://doi.org/10.1130/0091-7613(1998)026<0267:TPCOTB>2.3.CO;2.

Patriat, P., and Courtillot, V., 1984, On the stability of triple junctions and its relation to episodicity in spreading: Tectonics, v. 3, p. 317–332, https://doi.org/10.1029/TC003i003p00317.

Sandwell, D.T., Müller, R.D., Smith, W.H.F., Garcia, E., and Francis, R., 2014, New global marine gravity model from CryoSat-2 and Jason-1 reveals buried tectonic structure: Science, v. 346, p. 65–67, https://doi.org/10.1126/science.1258213.

Searle, R.C., and Francheteau, J., 1986, Morphology and tectonics of the Galapagos Triple Junction: Marine Geophysical Researches, v. 8, p. 95–129.

Schouten, H., Smith, D.K., Montési, L.G.J., Zhu, W., and Klein, E.M., 2008, Cracking north of the Galápagos triple junction: Geology, v. 36, p. 339–342, https://doi.org/10.1130/G24431A.1.

Sutherland, R., 1995, The Australia-Pacific boundary and Cenozoic plate motions in the SW Pacific: Some constraints from Geosat data: Tectonics, v. 14, p. 819–831, https://doi.org/10.1029/95TC00930.

Viso, R.F., Larson, R.L., and Pockalny, R.A., 2005, Tectonic evolution of the Pacific–Phoenix–Farallon triple junction in the South Pacific Ocean: Earth and Planetary Science Letters, v. 233, p. 179–194, https://doi.org/10.1016/j.epsl.2005.02.004.

Wessel, P., and Kroenke, L.W., 2008, Pacific absolute plate motion since 145 Ma: An assessment of the fixed hot spot hypothesis: Journal of Geophysical Research: Solid Earth, v. 113, B06101, https://doi.org/10.1029/2007JB005499.

Printed in USA